Macromolecules **1998,** *31,* 8878−8885

Thermoreversible Hydrogel of Short-Chain *O*-(2,3-Dihydroxypropyl)cellulose/Borax Aqueous Solution. Microscopic versus Macroscopic Properties

Nobuhiro Ide, Takaya Sato,† Takeaki Miyamoto, and Takeshi Fukuda*

Institute for Chemical Research, Kyoto University, Uji, Kyoto 611-0011, Japan

Received April 6, 1998

ABSTRACT: The thermoreversible hydrogel of short-chain (unentangled) *O*-(2,3-dihydroxypropyl)cellulose/Borax aqueous solution was studied by ^{11}B NMR and dynamic viscoelastic measurements. The total number X_T of transient cross-links formed by the (diol/ion) 2/1 complexation could be quantitatively estimated by ^{11}B NMR. The dynamic viscoelastic data gave the number N_E of elastically effective chains and the relaxation time of the gel. The N_E vs X_T data were compared to the mean-field theory of transient gels. Agreement between the theory and experiment was very poor at low C but became better as C increased. It was suggested that the ratio of the experimental N_E to the theoretical N_E is a function only of polymer concentration C. The gel point estimated by the zero extrapolation of the experimental N_E vs X_T data with a fixed C reasonably agreed with the mean-field prediction only at high C. The relaxation time τ (and hence the viscosity η) of the gel strongly depended on the pH of the system but not explicitly on C or on X_T (or N_E). For example, the value of τ observed for a solution at pH = 13.5 was more than 100 times as large as that observed for a similar solution at pH = 8.4, whereas the plateau moduli of the two solutions were similar in order of magnitude. It was suggested that τ in this system can be simply identified with the lifetime τ_0 of the transient cross-links.

Introduction

A large number of studies have been carried out on the hydrogel formation of polyhydroxyl polymers such as poly(vinyl alcohol) (PVA),[1−14] polysaccharides,[15−18] and poly(glyceryl methacrylate)[19] in the presence of metal ions or anionic species such as borate, titanate, and antimonate. In these systems, the complexes formed between such ions and hydroxyl groups on the polymer chains work as cross-links.

These hydrogels are transient by nature because the cross-links have a finite lifetime τ_0.[20,21] The gel point of such a system determined by a mechanical method is always time-dependent, which means that it is more like the glass transition temperature. When the time scale of observation is sufficiently shorter than τ_0, the dissociation−association process of the transient cross-link cannot be "seen", and accordingly, the system will be indistinguishable from a chemically cross-linked gel, both statically and dynamically. When the time scale of observation is comparable to or longer than τ_0, the relaxation process of the gel can be observed and characterized by a relaxation time, like a viscoelastic liquid. Several theories have dealt with the relaxation behavior of transient gels without[22−24] and with[25,27] entanglements. (Reference 25 actually deals with entangled polymer melts rather than reversible networks formed by complexation.) For an entangled gel, two maxima in the dynamic loss modulus G'' were observed: the low-frequency maximum corresponding to the longest relaxation time and the high-frequency one to the lifetime of the transient cross-link, τ_0.[28] The longest relaxation time τ is determined by the diffusional motion of the chain in an entanglement network reversibly forming cross-links with the surrounding chains. In this regard, τ of an entangled system is not a simple parameter to interpret quantitatively.[26,27]

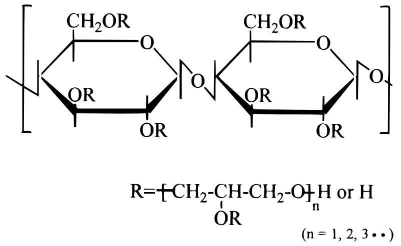

Figure 1. Chemical structure of *O*-(2,3-dihydroxypropyl)cellulose (DHPC).

This work deals with the hydrogels formed by a short-chain *O*-(2,3-dihydroxypropyl)cellulose (DHPC; Figure 1) in the presence of Borax ($Na_2B_4O_7 \cdot 10H_2O$).[18] DHPC is a water-soluble cellulose derivative with 1,2-diol sites in the side chains. Borax is a source of borate anion, and the complexation proceeds according to Scheme 1.[18] Here, the abbreviations B, B^-, A, AB^-, and A_2B^- denote $B(OH)_3$, $^-B(OH)_4$, free diol, and diol/borate anion complexes with 1/1 and 2/1 stoichiometry, respectively. This system has several advantages for fundamental studies on transient networks. First, the polymer chains are cross-linked solely by the 2/1 complex A_2B^-, and the concentration of A_2B^- or the total number X_T of cross-links per unit volume can be determined quantitatively by ^{11}B nuclear magnetic resonance spectroscopy (^{11}B NMR).[18] Second, the intramolecular cross-linking or loop formation, which does not contribute to the mechanical strength of the gel, will be largely suppressed due to the rigid-chain nature of cellulose backbone. Third, the system will be free from the complications caused by entanglements owing to the short-chain polymer used as a sample.

By studying this rather ideally simple system by means of ^{11}B NMR and dynamic rheometry, we wish to

---

† Present address: Nisshinbo Industries, Inc., Tokyo Research Center, Nishiarai-Sakaecho, Adachi-ku, Tokyo 123-0843, Japan.

10.1021/ma9805351 CCC: \$15.00

Scheme 1

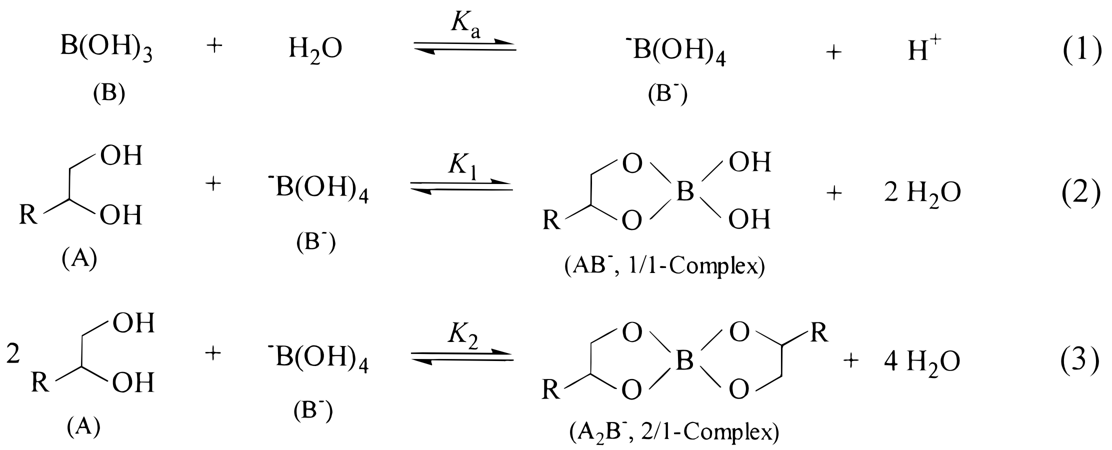

give a new and deep insight into the classical but still not well understood problems regarding the relationships between the microscopic properties of a transient gel such as the density and lifetime of cross-link and its macroscopic properties such as the gel point, the plateau modulus, and the longest relaxation time τ. The rheological method has already been used by some authors[11,14] to determine the number of elastically effective cross-links, X_E, of a hydroxyl polymer/Borax system; however, the total number of cross-links, X_T, has never been directly determined at the same time. In this study, the combined use of the NMR and rheological methods has allowed us to determine both X_T and X_E and thereby to make a (virtually first) comprehensive comparison between experiments and theories, specifically, the mean-field theories on transient gels.[29-32]

Experimental Section

Materials. DHPC was prepared by reaction of cellulose with 2,3-epoxy-1-propanol in a 10 wt % LiCl−dimethylacetamide homogeneous solution, as described previously.[18] The number-average molecular weight M_n and the polydispersity index M_w/M_n was 17 000 and 2.3, respectively. The number f_n of 1,2-diol sites per polymer chain determined by NMR was 48. (See ref 18 for details of the NMR analysis.) A stock sample solution was prepared by dissolving an appropriate amount of DHPC in deionized water with stirring at room temperature, to which Borax was added, and the mixture was heated and stirred at 80 °C to obtain a homogeneous solution. When necessary, NaOH (or HCl) was added to adjust the pH of the solution.

^{11}B NMR Measurements. ^{11}B NMR spectra were recorded at 10 °C with a JEOL JNM-AL400 Fourier transform spectrometer operating at 127.0 MHz for ^{11}B nuclei, using a 5 mm o.d. quartz tube. ^{11}B chemical shifts were determined relative to the external $BF_3O(C_2H_5)_2$ standard. Sample solutions were prepared according to the same procedure as described above, except that a mixture of deionized and deuterated water was used as solvent.

Dynamic Rheometry. Rheological measurements were performed on a dynamic stress-controlled rheometer, SR-200 (Rheometrics, Inc., Piscataway, NJ). A cone-plate geometry with a cone diameter of 25.0 mm and cone angle of 0.0989 rad was used. After the solution was loaded into the rheometer, a sufficient time (about 30 min) was allowed for the solution to relax and achieve thermal equilibrium. Measurements were made at various temperatures ranging from 0 to 30 °C with 0.1 °C accuracy with a humidity cover used to prevent solvent evaporation. Stress sweep experiments were performed within the linear viscoelastic region, where moduli were independent of stress, and the flow was confirmed to be reproducible even after many measurements. The storage modulus G' and the loss modulus G'' were monitored as a function of the angular frequency ω from 0.1 to 100 rad s^{-1}.

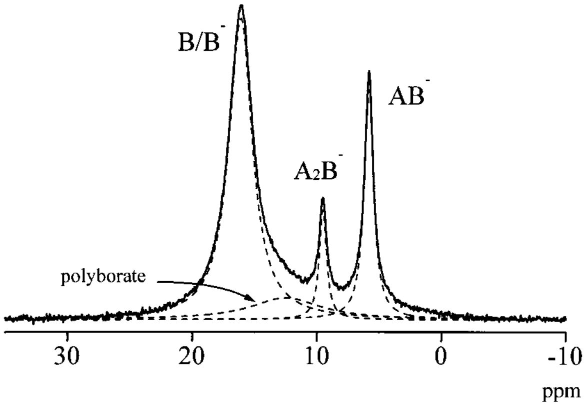

Figure 2. ^{11}B NMR spectrum of a sample solution (C = 84 g L^{-1} and $[B_T]$ = 0.10 mol L^{-1}) at 10 °C. The spectrum can be resolved into the four Lorentzian components shown by the broken lines (see text).

Time−Temperature Superposition. Time−temperature superposition was performed by using the Rheometrics software RHIOS. This program determines the vertical and horizontal shift factors at each temperature by minimizing the mean-square deviations between the shifted and reference curves.

Results

^{11}B NMR Measurements. Figure 2 shows the ^{11}B NMR spectrum of a sample solution (C = 84 g L^{-1} and $[B_T]$ = 0.10 mol L^{-1}) at 10 °C. The spectrum can be resolved into the four Lorentzian peaks assignable to boric acid (B)/borate anion (B^-), A_2B^-, AB^-, and polyborate species, respectively.[18] The polyborate species formed by the multiequilibrium reactions of borate anions[33] were detectable only when $[B_T]$ was larger than about 0.1 M. The chemical shift of the B/B^- combined signal strongly depended on pH, which means that pH has a strong influence on the equilibration of these two species.[3] In other words, we could use this chemical shift to determine the pH of the system. In some samples, $[A_2B^-]$ and pH were evaluated indirectly by solving the equilibrium equations.[18] These calculated values well agreed with the measured ones. The values of $[A_2B^-]$ ($=X_T$), α, and pH are tabulated in Tables 1−3, where α is the fraction of the diol sites participating in the A_2B^- complexation (fraction of cross-linked diol sites), which is given by $\alpha = 2[A_2B^-]/[A_T]$, where $[A_T]$ is the total concentration of diol sites.

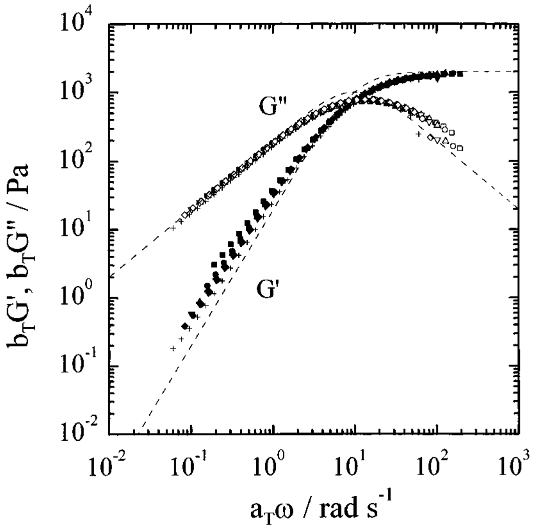

Figure 3. Storage (G') and loss (G'') moduli vs frequency (ω) master curves for a DHPC/Borax solution ($C = 84$ g L^{-1} and [B$_T$] = 0.10 mol L^{-1}: reference temperature = 10 °C). Broken curves show the Maxwellian model, and a_T and b_T are the horizontal and vertical shift factors, respectively: temperature (°C) = (■, □) 0.7; (●, ○) 3.5; (▲, △) 6.6; (▼, ▽) 9.7; (◆, ◇) 12.4; (+) 15.1.

Viscoelastic Measurements. Figure 3 shows the storage and loss moduli, G' and G'', of DHPC/Borax aqueous solution at 10 °C as a function of frequency ω. (In the figure, the data obtained at other temperatures are superposed on the 10 °C data, as will be described later on.) At low frequencies, $G'(\omega)$ and $G''(\omega)$ are proportional to ω^2 and ω, respectively, and at high frequencies, a plateau zone in $G'(\omega)$ and a marked maximum in $G''(\omega)$ are observed. The broken lines in the figure show the Maxwell model (eqs 4 and 5) with the relaxation time $\tau = \omega_{\max}{}^{-1}$, where $\omega_{\max}$ is the angular frequency at which G'' is maximum:

$$G'(\omega) = G_N\omega^2\tau^2/(1 + \omega^2\tau^2) \tag{4}$$

$$G''(\omega) = G_N\omega\tau/(1 + \omega^2\tau^2) \tag{5}$$

The plateau modulus G_N is the value of G' in the plateau zone at high frequencies. The applicability of this model became somewhat poorer with increasing polymer concentration C.[11,14] The relaxation time τ ($=\omega_{\max}{}^{-1}$) could be determined for all studied solutions with $C \leq 135$ g L^{-1}.

In the simplest theory of transient networks, G_N is written[22]

$$G_N = N_{E,\exp}kT \tag{6}$$

where k is the Boltzmann constant and T is the absolute temperature. The number density of elastically effective network chains, $N_{E,\exp}$, is experimentally evaluated from G_N by using eq 6. The values of G_N, $N_{E,\exp}$, and τ are tabulated in Table 3.

A plateau modulus was observed only when the polymer concentration C was sufficiently high *and* the borate concentration [B$_T$] exceeded a certain value that apparently depended on C. We also note that even the solution with C as high as 190 g L^{-1} showed no measurable magnitude of G' when no Borax was added to the system. ($G' \approx 10^{-3}$ Pa was the lower limit of G' measurable by this experimental setup.) These results reasonably suggest some qualitative features of this (and similar) system(s). First, gelation does not take place unless C is large enough so that polymer chains overlap with each other to a sufficient degree. When C is sufficiently large, *and* the number of the transient cross-links produced by the ionic complexation is sufficiently large, the system behaves as a gel in a high-ω region to give a plateau modulus. The modulus contains no contribution from entanglements (owing to the short-chain nature of the present DHPC sample). Like in a chemically cross-linked gel, there must be a critical threshold of gelation (gel point) in such a transient network, too, but it may not be easy to determine it directly. We will come back to this point later on.

Viscoelastic Behavior at Various pH. Figure 4 shows $G'(\omega)$ and $G''(\omega)$ of the samples with $C = 84$ g L^{-1}, [B$_T$] = 0.1 mol L^{-1}, and varying pH (10 °C). The cross-link formation or the reaction between a pair of diol sites and borate anion is pH-dependent so that X_T varies by addition of a small amount of NaOH (or HCl). However, in the series of solutions with $C = 84$ g L^{-1} and [B$_T$] = 0.1 mol L^{-1} (codes 7-1 through 7-4), X_T varied only by a factor of 3 when pH changed from 8.0 to 13.3. On the other hand, τ showed a variation of more than 2 orders of magnitude for the same change in pH (Tables 2 and 3). In accordance with this variation of τ, the viscosity η of some DHPC/Borax solutions dramatically increased (by more than 2 orders of magnitude) with an increase in pH (see Table 3).

Discussion

Plateau Modulus G_N: Comparison with Theories. In many previous reports,[2,11,16,17] the plateau modulus G_N and hence the number density of elastically effective chains, $N_{E,\exp}$ (eq 6), were assumed to be proportional to the total cross-link density X_T, i.e.,

$$N_{E,\exp} \approx 2X_T \tag{7}$$

However, the present study, in which both G_N and X_T were determined, clearly reveals that eq 7 does not hold, as demonstrated in Figure 5. All data points lie below the broken line given by eq 7. This is quite reasonable, since X_T generally includes not only elastically effective cross-links but also elastically ineffective ones forming loops or pendent chains in the gel fraction or existing in the sol fraction. Figure 5 indicates that the fraction of elastically effective chains is generally very small: when X_T is fixed, $N_{E,\exp}$ increases with increasing C, and when C is fixed, $N_{E,\exp}$ varies such as $X_T{}^2$. The values of $N_{E,\exp}$ observed at varying values of pH (the open symbols in the figure) fall on the same line (with the same C). This suggests that G_N is a function of C and X_T, only, in marked contrast to the behavior of the viscosity η, which strongly depends on pH (see below).

The theory of gelation originated by Flory and Stockmayer (FS)[34,35] has been extended to reversible networks by many workers.[29−32,36−38] In these theories a model network is constructed, in the mean-field approximation, from a number density N_0 of primary chains, each having f functional groups capable of reversibly forming aggregates with multiplicity m. For $m = 2$ (pairwise aggregation like in the present system), the density $N_{E,\text{theo}}$ of elastically effective chains as a function of f

Table 1. Results of ^{11}B NMR Measurements (10 °C)

solution code	C, g L^{-1}	[borate], mol L^{-1}	pH	[A_2B^-], mol L^{-1}	[AB^-], mol L^{-1}	[B^-], mol L^{-1}	[B], mol L^{-1}	[PB], mol L^{-1}
1-1	59	0.10	8.5	8.0×10^{-3}	1.9×10^{-2}	2.0×10^{-2}	5.4×10^{-2}	0
1-2	59	0.15	8.6	1.2×10^{-2}	2.4×10^{-2}	3.2×10^{-2}	8.2×10^{-2}	0
1-3	59	0.20	8.8					
2-1	70	0.05	8.3	5.3×10^{-3}	1.0×10^{-2}	5.8×10^{-3}	2.9×10^{-2}	0
2-2	70	0.10	8.4	9.0×10^{-3}	2.0×10^{-2}	1.5×10^{-2}	5.6×10^{-2}	0
2-3	70	0.15	8.6	1.4×10^{-2}	2.7×10^{-2}	2.4×10^{-2}	6.6×10^{-2}	1.8×10^{-2}
3-1	84	0.05	8.3	5.3×10^{-3}	1.1×10^{-2}	2.9×10^{-3}	3.1×10^{-2}	0
3-2	84	0.10	8.4	9.7×10^{-3}	1.9×10^{-2}	1.0×10^{-2}	4.8×10^{-2}	1.4×10^{-2}
4-1	108	0.05	8.1	5.3×10^{-3}	1.1×10^{-2}	3.4×10^{-3}	3.1×10^{-2}	0
4-2	108	0.10	8.2	9.0×10^{-3}	2.1×10^{-2}	8.5×10^{-3}	5.6×10^{-2}	5.9×10^{-3}
4-3	108	0.15	8.4	1.5×10^{-2}	2.9×10^{-2}	1.7×10^{-2}	8.1×10^{-2}	9.5×10^{-3}
4-4	108	0.20	8.4	2.3×10^{-2}	4.6×10^{-2}	2.1×10^{-2}	9.7×10^{-2}	1.2×10^{-2}
5-1	135	0.05	7.9	6.2×10^{-3}	8.5×10^{-3}	2.4×10^{-3}	3.3×10^{-2}	0
5-2	135	0.10	8.0	1.1×10^{-2}	2.1×10^{-2}	4.4×10^{-3}	5.9×10^{-2}	4.4×10^{-3}
5-3	135	0.15	8.2	1.8×10^{-2}	3.1×10^{-2}	1.1×10^{-2}	7.9×10^{-2}	1.2×10^{-2}
6-1	158	0.03	8.2[a]	3.6×10^{-3} [a]				
6-2	158	0.05	7.5	6.0×10^{-3}	1.1×10^{-2}	2.5×10^{-3}	3.1×10^{-2}	0
6-3	158	0.10	7.9	9.5×10^{-3}	2.0×10^{-2}	4.6×10^{-3}	5.8×10^{-2}	8.4×10^{-3}

[a] Calculated as detailed in ref 18b.

Table 2. Values of [A_2B^-] at Various pH (10 °C)[a]

solution code	C, g L^{-1}	[borate], mol L^{-1}	[NaOH] (or [HCl]), mol L^{-1}	pH	[A_2B^-], mol L^{-1}
7-1	84	0.10	0.030[b]	8.0	5.4×10^{-3}
7-2	84	0.10	0.030	9.6	1.6×10^{-2}
7-3	84	0.10	0.060	12.8	1.7×10^{-2}
7-4	84	0.10	0.10	13.3	1.7×10^{-2}
8-1	135	0.10	0.030[b]	7.7	6.3×10^{-3}
8-2	135	0.10	0.015[b]	7.9	1.0×10^{-2}
8-3	135	0.10	0.025	9.0	2.0×10^{-2}
8-4	135	0.10	0.050	12.0	2.4×10^{-2}
9-1	60	0.011	0.1	13.5	2.4×10^{-3}
9-2	60	0.022	0.1	13.5	4.8×10^{-3}
9-3	60	0.051	0.1	13.4	8.8×10^{-3}
9-4	60	0.12	0.1	13.2	1.3×10^{-2}
10-1	80	0.012	0.1	13.5	3.5×10^{-3}
10-2	80	0.020	0.1	13.5	5.7×10^{-3}
10-3	80	0.049	0.1	13.4	1.2×10^{-2}
10-4	80	0.096	0.1	13.3	1.9×10^{-2}

[a] Calculated as detailed in ref 18b. [b] Concentration of HCl.

and the fraction α of reacted groups reads[29,30,32]

$$\frac{N_{\mathrm{E,theo}}}{\alpha f N_0} = \left[1 - 2x + \frac{1 + \alpha x}{\alpha f}\right]\left[1 + x - \frac{2(1 + \alpha x)}{\alpha f}\right] \quad (8)$$

where x is the lowest positive root of the equation

$$x = (1 - \alpha + \alpha x)^{f-1} \quad (9)$$

Equations 8 and 9 were originally derived by Langley and Polmanteer.[29] They are valid for monodisperse primary chains. At the moment, there is no published theory that is applicable to polydisperse primary chains. We tentatively adopt eqs 8 and 9 with the functionality f given by the weight-average value f_w (=110 for our DHPC sample). This seems to be a reasonable choice, since it is consistent at least with the known gel point for polydisperse systems[34,35]

$$\alpha_g = (f_w - 1)^{-1} \quad (10)$$

where subscript "g" denotes the gel point. Naturally, the comparison between the theory and experiments should be made for common values of X_T (=$\alpha f_n N_0/2$), and hence the use of f_w automatically redefines the value of N_0 to be used in the theory.

Table 3. Results of Dynamic Rheometry (10 °C)

solution code	α[a]	G_N, Pa	$N_{E,exp}$, mol L^{-1}	$10^2\tau$, s	η, Pa s
1-1	0.096	85	3.6×10^{-5}	3.3	2.9
1-2	0.144	210	8.9×10^{-5}	4.8	13
1-3		360	1.5×10^{-4}	5.9	26
2-1	0.054	300	1.3×10^{-4}	4.1	
2-2	0.091	930	4.0×10^{-4}	5.0	67
2-3	0.142	2000	8.5×10^{-4}	7.1	100
3-1	0.045	520	2.2×10^{-4}	5.0	31
3-2	0.082	1800	7.7×10^{-4}	6.9	200
4-1	0.035	1100	4.7×10^{-4}	3.4	34
4-2	0.059	3800	1.6×10^{-3}	6.5	420
4-3	0.099	8800	3.7×10^{-3}	7.1	1300
4-4	0.151	16000	6.8×10^{-3}	9.3	2600
5-1	0.033	3400	1.4×10^{-3}	4.3	270
5-2	0.058	15000	6.4×10^{-3}	5.9	2200
5-3	0.095	30000	1.3×10^{-2}	10	6000
6-1	0.016	2000	8.5×10^{-4}		
6-2	0.027	8000	3.4×10^{-3}		660
6-3	0.043	30000	1.3×10^{-2}		5300
7-1	0.046	500	2.1×10^{-4}	1.4	19
7-2	0.135	3200	1.4×10^{-3}	18	700
7-3	0.144	3900	1.7×10^{-3}	48	2800
7-4	0.144	5000	2.1×10^{-3}	410	
8-1	0.033	4100	1.7×10^{-3}	1.6	110
8-2	0.053	7300	3.1×10^{-3}	2.7	320
8-3	0.105	29000	1.2×10^{-2}	16	9200
8-4	0.126	29000	1.2×10^{-2}	38	23000
9-1					
9-2					
9-3	0.104	300	1.3×10^{-4}	670	
9-4	0.154	400	1.7×10^{-4}	500	
10-1					
10-2	0.051	740	3.1×10^{-4}	1000	
10-3	0.107	2400	1.0×10^{-3}	630	
10-4	0.169	3800	1.6×10^{-3}	320	

[a] Fraction of cross-linked diol sites: $\alpha = 2[X_T]/[A_T]$, where $[X_T] = [A_2B^-]$ and $[A_T] = Cf_n/M_n$ with $F_n = 48$ and $M_n = 17\,000$.

Figure 6 shows the comparison between $N_{E,exp}$ and $N_{E,theo}$ (eq 8). Clearly, experimental points mostly lie far below the theoretical line, indicating the failure of the mean-field approach particularly for low-C solutions. Interestingly, the experimental points with a fixed value of C are approximately linear in all cases. This suggests a useful method for experimentally determining the gel point of a transient network. The method works at arbitrary C if G_N is measurable. Even though data points are not many enough to give accurate values of α at the gel point (α_g), the α_g determined in this way apparently depends on C: as C increases, α_g decreases,

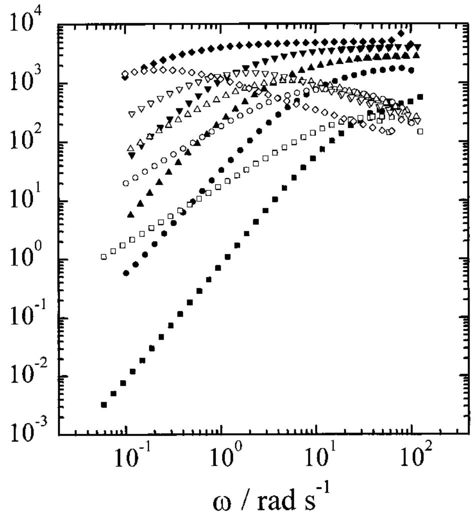

Figure 4. Storage (filled symbols) and loss (open symbols) moduli of a DHPC/Borax solution (10 °C) as a function of frequency ω ($C = 84$ g L^{-1} and $[B_T] = 0.10$ mol L^{-1}): pH = (■) 8.0; (●) 8.4; (▲) 9.6; (▼) 12.8; (◆) 13.3.

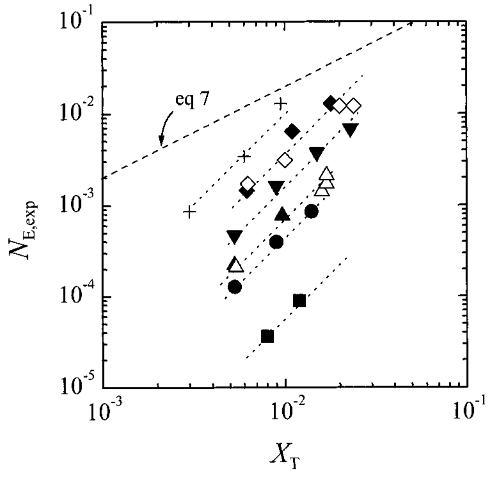

Figure 5. Plot of $N_{E,exp}$ vs X_T for DHPC/Borax solutions (10 °C). Polymer concentrations (g L^{-1}): (■) 59; (●) 70; (▲, △) 84; (▼) 108; (◆, ◇) 135; (+) 158. The solutions shown by the open symbols (△ and ◇) contain NaOH (or HCl) to adjust pH. The slopes of dotted lines are 2. The broken line shows the relation $N_E = 2X_T$.

coming closer to the mean-field value of α_g ($=f_w^{-1} = 0.009$). This trend is consistent with our previous results,[18b,39,40] indicating that the mean-field theory becomes a valid approximation only at sufficiently high concentrations. At low concentrations, the spatial distribution of polymer segments is not homogeneous enough for the mean-field treatment to be applicable. Indeed, the present work also shows that $N_{E,exp}$ is seriously different from the mean-field prediction $N_{E,theo}$, especially at low C (Figure 6).

The difference (of a factor about 2) in the critical value α_g observed between the theory and the highest-C data is believed to be real and originate, at least partly, in the neglect of loops in the theory. We recently observed a similar magnitude of difference between the theoretical and experimental gel points for a highly concentrated *model* system ($C \geq 500$ g L^{-1}),[40] in which the cross-linking reaction proceeds nearly randomly or the spatial distribution of reactants is nearly homogeneous.[41]

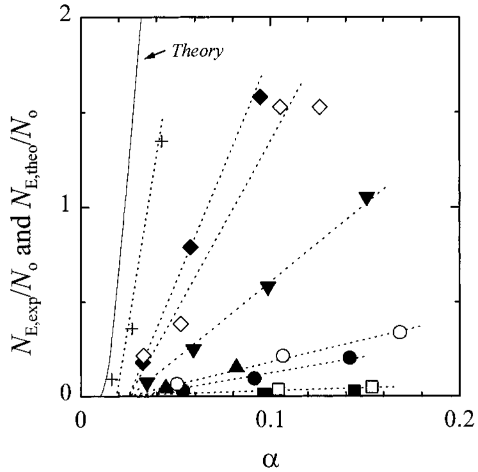

Figure 6. Plot of $N_{E,exp}/N_0$ vs α (10 °C). Polymer concentrations (g L^{-1}): (■) 59; (□) 60; (●) 70; (○) 80; (▲) 84; (▼) 108; (◆, ◇) 135; (+) 158. The solutions shown by the open symbols (□, ○, and ◇) contain NaOH (or HCl) to adjust pH. The solid line represents the mean-field theory (eq 8), and the dotted lines are for the eye.

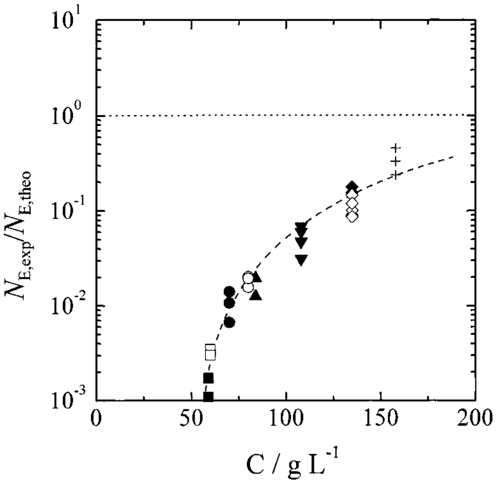

Figure 7. Plot of $N_{E,exp}/N_{E,theo}$ vs polymer concentration C (10 °C) for the data given in Figure 6. See the caption to Figure 6 for symbols.

Figure 7 shows the ratio of $N_{E,exp}$ to $N_{E,theo}$ as a function of C. Clearly, all the data form a single master curve, indicating that the validity of the mean-field theory depends primarily on C: the higher is C, the more valid is the theory. The master curve appears to approach the ratio of unity at high C, indicating that the mean-field theory may be fully justified at sufficiently high concentrations. However, this cannot be concluded because the validity of eqs 8 and 9 with the weight-average f value is still questionable in a rigorous sense and because the validity of eq 6 (with the "front factor" assumed to be unity) is also unclear. We would rather believe that even in the high-C limit, the actual number of elastically effective chains may be somewhat smaller than the mean-field value (say, $N_{E,exp}/N_{E,theo} \approx 0.5$, as already implied) due to the inevitable formation of elastically ineffective loops. In any case, we may safely conclude from the present results that the mean-field theory becomes a valid approximation only at sufficiently high concentrations, in accordance with previous conclusions.[18b,39,40] Figure 7 also suggests that gelation does not take place at concentrations below about 50 g L^{-1}. This critical concentration C_c is about twice as large as the overlap concentration C^*, which defines the threshold between the dilute and semidilute solutions and is approximated here by the relation $C^* = [\eta]^{-1}$ to be 26 g L^{-1}, where $[\eta]$ is the intrinsic viscosity of the DHPC sample in Borax-free water.

Since the results given in this section are concerned with the plateau modulus of the gel, the other important aspect of the gel, i.e., the thermoreversibility, does not explicitly appear. In this relation, comments may be due on a recent interesting publication by Takada et al.,[14] who dealt with the gelation of poly(vinyl alcohol)/Borax aqueous solutions. In that work, they also estimated N_E by the rheological method: using the α vs N_0 relation,[31,32] originally due to Clark and Ross-Murphy[31]

$$\alpha = [1 + 2z - (1 + 4z)^{1/2}]/(2z) \qquad (11)$$

$$z = KN_0f \qquad (12)$$

with K being an equilibrium constant of the pairwise association of the functional units of the polymer; these authors plotted N_E/N_0 as a function of the scaled concentration $(\phi - \phi_g)/\phi_g$ $[=(N_0 - N_{0,g})/N_{0,g}]$, where ϕ is the polymer volume fraction with the subscript g denoting the gel point, and they estimated ϕ_g (or $N_{0,g}$) by the viscometric method. The experimental data well reproduced the theoretical curve computed from eqs 8–10 with eqs 11 and 12. (Actually, the experimental points lay somewhat *above* the theoretical curve.) In this regard, their results are not consistent with ours. However, the fair agreement between the theories and experiments noted by them should be viewed with reserve, since in their work the theoretical eqs 8, 10, and 11 were tested not individually but in combination. Errors of different origins could cancel each other, leading to an apparent success of the combined theoretical relation. We would like to comment that the use of eqs 11 and 12 with N_0-independent K may be inaccurate for a hydroxyl polymer/Borax system, where α is known to be a complicated function of polymer and Borax concentrations,[18] and that the gel point determined by the viscometric method[14] may not accurately correspond to eq 10, as suggested above and also by the work of Sato et al.,[18] who used the tube-inverting method to determine the gel point.

Temperature Dependence of G_N and τ. G_N and τ of this system depended on temperature. Since the pH of the system without added NaOH (or HCl) was nearly constant in the studied temperature range (0–30 °C), the observed temperature dependence of G_N and τ comes mainly from the variation of the equilibrium constants with temperature. Examples of the G' and G'' vs ω master curves were already shown in Figure 3, which includes experimental data, collected at various temperatures, superimposed by shifting both horizontally and vertically according to

$$b_TG'(\omega,T) = (T/T_{ref})G'(a_T\omega,T_{ref}) \qquad (13)$$

$$b_TG''(\omega,T) = (T/T_{ref})G''(a_T\omega,T_{ref}) \qquad (14)$$

where a_T and b_T are the horizontal and vertical shift factors, respectively, and T_{ref} is the reference temperature (10 °C, in this work). For the DHPC/Borax aqueous system, this superposition appears to be valid at least in the studied range of C. Within the studied range of temperature, the shift factors could be fitted to the Arrhenius type equations

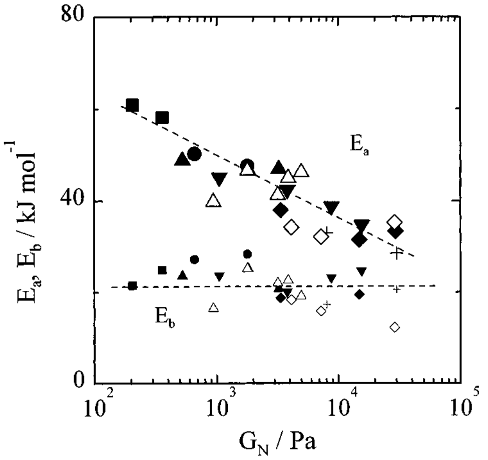

Figure 8. Plot of activation energies E_a (large symbols) and E_b (small symbols) vs elastic plateau modulus G_N at 10 °C. Polymer concentrations (g L^{-1}): (■) 59; (●) 70; (▲, △) 84; (▼) 108; (◆, ◇) 135; (+) 158. The solutions shown by the open symbols (△ and ◇) contain NaOH (or HCl) to adjust pH.

$$a_T = \exp[E_a/R(T^{-1} - T_{ref}^{\ -1})] \qquad (15)$$

$$b_T = \exp[-E_b/R(T^{-1} - T_{ref}^{\ -1})] \qquad (16)$$

The activation energies E_a and E_b obtained for various values of C are plotted as a function of G_N in Figure 8. The energy E_a tends to decrease from 61 to 29 kJ mol^{-1}, while G_N increases from about 200 to 30 000 Pa, regardless of the concentrations of polymer and Borax and pH. On the other hand, the energy E_b is approximately constant (≈21 kJ mol^{-1}), independent of polymer and Borax concentrations and pH. This value of E_b is consistent with the enthalpies of gelation estimated from the gel melting temperatures[42] of the Borax solutions of DHPC (26 kJ mol^{-1})[18b] and poly(vinyl alcohol) (20–44 kJ mol^{-1}).[8] This value is also close to the enthalpy changes of diol–borate dicomplexation determined by ^{11}B NMR for DHPC (22 kJ mol^{-1})[18a] and other hydroxyl polymers (14–34 kJ mol^{-1}).[3,15] However, the real reason for the reasonable agreement of the activation energies obtained by the spectroscopic and mechanical measurements is not necessarily clear, since the relationships between the microscopic and macroscopic properties are not so simple, as we have seen.

Gel Relaxation Time τ and Cross-Link Lifetime τ_0. As already mentioned, the present system with the short-chain DHPC should be essentially free from any effects of chain entanglement, and hence G_N and τ should be a function only of the effective number and lifetime of cross-links. Figure 9 shows the plots of τ vs X_T and $N_{E,exp}$. Open and filled symbols are for solutions with and without NaOH, respectively. In both cases, τ appears to be independent of polymer concentration and slightly increases (in the absence of NaOH) or decreases (in the presence of NaOH) with increasing X_T (or $N_{E,exp}$). One would have expected that as X_T and hence $N_{E,exp}$ increase, τ would increase, since a chain with many constraints (cross-links) will be slower to relax than the one with fewer constraints. This seemingly is the case with the NaOH-free (approximately neutral) solutions. However, the reverse is the case with the NaOH-added (high pH) solutions. The enormous differences in τ between the two groups of solutions with the same

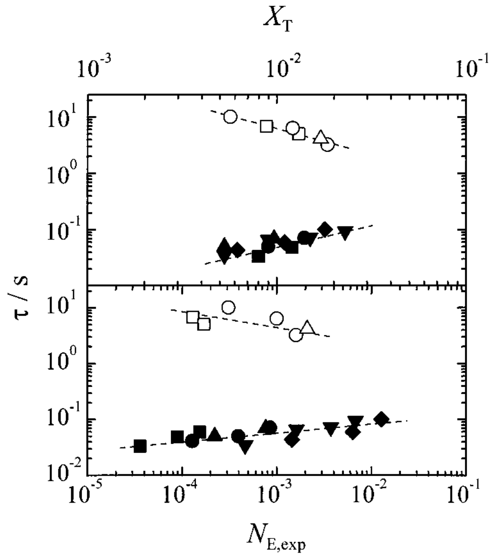

Figure 9. Plot of τ vs (a) X_T and (b) $N_{E,exp}$ at 10 °C. Polymer concentrations (g L^{-1}): (■) 59; (□) 60; (●) 70; (○) 80; (▲, △) 84; (▼) 108; (◆) 135. The solutions shown by the open symbols (□, ○, and △) contain NaOH (or HCl) to adjust pH.

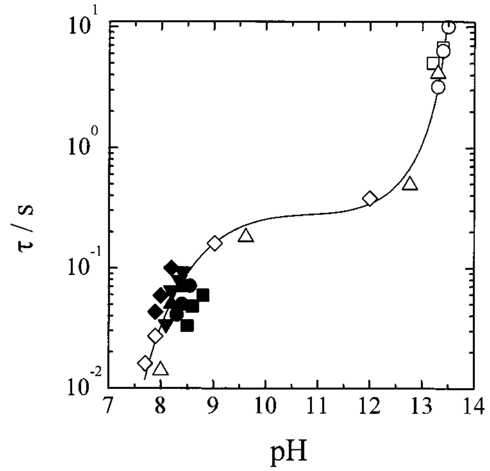

Figure 10. Plot of τ vs pH at 10 °C. Polymer concentrations (g L^{-1}): (■) 59; (□) 60; (●) 70; (○) 80; (▲, △) 84; (▼) 108; (◆, ◇) 135. The solutions shown by the open symbols (□, ○, △, and ◇) contain NaOH (or HCl) to adjust pH.

values of $N_{E,exp}$ (cf. Figure 9) suggest that the effect of multiple cross-links along the chain on τ is minor at least in the studied range of $N_{E,exp}$, where $N_{E,exp}$ is no greater than a few effective cross-links per chain. Moreover, the dependence of τ on $N_{E,exp}$ observed even in the region $N_{E,exp} < 10^{-3}$, where the average number of effective cross-links per chain is much less than one, strongly indicates that the dependence arises from a different origin.

Figure 10 shows the plot of τ against pH. All the data points are well represented by the master curve given by the solid line in the figure. This suggests that we can identify τ with the cross-link lifetime τ_0 with no serious error, and the observed (apparent) dependence of τ on $N_{E,exp}$ can be interpreted in terms of the pH dependence of τ_0. The scattering of the data points around pH = 8 is ascribed to experimental uncertainties in pH and/or τ rather than to other specific causes. In previous studies on poly(glyceryl methacrylate)/Borax systems, the equilibrium constant K_2 of the (diol/borate) 2/1 complexation was estimated to be about 15 at pH = 12 by Pezron et al.[19] and about 20 at pH = about 8 by us.[43] This suggests that K_2 does not largely depend on pH. The large values of τ at high pH, therefore, mean that both of the rates of complexation and decomplexation become extremely small at high pH. The reason or mechanism for this phenomenon remains to be clarified.

Conclusions

The thermoreversible gels of DHPC/Borax aqueous solutions were examined by ^{11}B NMR for the total density X_T of transient cross-links and by dynamic rheometry for the gel relaxation time τ and plateau modulus. The following results were obtained:

(1) There is a critical polymer concentration C_c below which the system shows no plateau modulus (hence no gelation). This concentration is some 50 g L^{-1}, about twice as large as the overlap concentration C^* estimated by $C^* = [\eta]^{-1}$.

(2) For $C > C_c$, the system shows a plateau modulus G_N when X_T and hence the fraction α of reacted (cross-linked) diol sites of DHPC exceeded a certain critical value. The density $N_{E,exp}$ of elastically effective chains was estimated from G_N and compared with the mean-field theoretical prediction, $N_{E,theo}$. The ratio $N_{E,exp}/N_{E,theo}$ was nearly independent of α but strongly dependent on C, especially when C was small. The ratio increased with increasing C, meaning that the mean-field theory becomes a valid approximation only at sufficiently large C.

(3) The critical α value of gelation estimated by the zero extrapolation of the $N_{E,exp}$ data was generally larger than the mean-field prediction, decreasing with increasing C, coming closer to the mean-field prediction within a factor about 2 at the highest C studied.

(4) The gel relaxation time τ (and hence the viscosity η) strongly depended on the pH of the solution but not explicitly on C and X_T, suggesting that the τ of this system may be identified with the cross-link lifetime τ_0. The strong dependence of τ (or η) on pH suggests a powerful and general means to adjust the viscosity of polyhydroxyl polymer solutions.

(5) The vertical shift factor of the G' and G'' vs ω data gave an estimation of the activation energy of gelation, which reasonably agreed with reported values estimated by different methods.

Acknowledgment. This work was supported by a Grant-in-Aid for Scientific Research from the Ministry of Education, Science and Culture, Japan (Grant-in-Aid 05453150).

References and Notes

(1) Savins, J. G. *Rheol. Acta* **1968**, *7*, 87.
(2) Schultz, R. K.; Myers, R. R. *Macromolecules* **1969**, *2*, 281.
(3) Sinton, S. W. *Macromolecules* **1987**, *20*, 2430.
(4) Maerker, J. M.; Sinton, S. W. *J. Rheol.* **1986**, *30*, 77.
(5) Leibler, L.; Pezron, E. In *Space-Time Organization in Macromolecular Fluids*; Tanaka, F., Doi, M., Ohta T., Eds.; Springer-Verlag: Berlin, 1989; p 85.
(6) Pezron, E.; Leibler, L.; Lafuma, F. *Macromolecules* **1989**, *22*, 2656.
(7) Shibayama, M.; Sato, M.; Kimura, Y.; Fujiwara, H.; Nomura, S. *Polymer* **1988**, *29*, 336.
(8) Shibayama, M.; Yoshizawa, H.; Kurokawa, H.; Fujiwara, H.; Nomura, S. *Polymer* **1988**, *29*, 2066.
(9) Kurokawa, H.; Shibayama, M.; Ishimaru, T.; Nomura, S.; Wu, W.-l. *Polymer* **1992**, *33*, 2182.

(10) Inoue, T.; Osaki, K. *Rheol. Acta* **1993**, *32*, 550.
(11) Koike, A.; Nemoto, N.; Inoue, T.; Osaki, K. *Macromolecules* **1995**, *28*, 2339.
(12) Nemoto, N.; Koike, A.; Osaki, K. *Macromolecules* **1996**, *29*, 1445.
(13) Robb, I. D.; Smeulders, J. B. A. F. *Polymer* **1997**, *38*, 2165.
(14) Takada, A.; Nishimura, M.; Koike, A.; Nemoto, N. *Macromolecules* **1998**, *31*, 436.
(15) (a) Pezron, E.; Ricard, A.; Lafuma, F.; Audebert, R. *Macromolecules* **1988**, *21*, 1121. (b) Pezron, E.; Leibler, L.; Ricard, A.; Audebert, R. *Macromolecules* **1988**, *21*, 1126.
(16) Pezron, E.; Ricard, A.; Leibler, L. *J. Polym. Sci., Polym. Phys. Ed.* **1990**, *28*, 2445.
(17) Kesavan, S.; Prud'homme, R. K. *Macromolecules* **1992**, *25*, 2026.
(18) (a) Sato, T.; Tsujii, Y.; Fukuda, T.; Miyamoto, T. *Macromolecules* **1992**, *25*, 3890. (b) Sato, T.; Tsujii, Y.; Fukuda, T.; Miyamoto, T. *Macromolecules* **1992**, *25*, 5970.
(19) Pezron, E.; Leibler, L.; Ricard, A.; Lafuma, F.; Audebert, R. *Macromolecules* **1989**, *22*, 1169.
(20) De Genne, P.-G. *Scaling Concepts in Polymer Physics*; Cornell University Press: Ithaca, NY, 1979.
(21) (a) Clark, A. H.; Ross-Murphy, S. B. *Adv. Polym. Sci.* **1987**, *83*, 57. (b) te Nijenhuis, K. *Adv. Polym. Sci.* **1997**, *130*, 1.
(22) Green, M. S.; Tobolsky, A. V. *J. Chem. Phys.* **1946**, *14*, 80.
(23) Baxandall, L. G. *Macromolecules* **1989**, *22*, 1982.
(24) Tanaka, F.; Edwards, S. F. *Macromolecules* **1992**, *25*, 1516.
(25) Yamamoto, M. *J. Phys. Soc. Jpn.* **1956**, *11*, 413; **1957**, *12*, 1148; **1958**, *13*, 1200.
(26) Gonzalez, A. E. *Polymer* **1984**, *25*, 1469.
(27) Leibler, L.; Rubinstein, M.; Colby, R. H. *Macromolecules* **1991**, *24*, 4701.
(28) (a) Stadler, R.; de Lucca Freitas, L. *Colloid Polym. Sci.* **1986**, *264*, 773. (b) Stadler, R. *Prog. Colloid Polym. Sci.* **1987**, *75*, 140. (c) de Lucca Freitas, L. L.; Stadler, R. *Macromolecules* **1987**, *20*, 2478.
(29) Langley, N. R.; Polmanteer, K. E. *J. Polym. Sci., Polym. Phys. Ed.* **1974**, *12*, 1023.
(30) Pearson, D. S.; Graessley, W. W. *Macromolecules* **1978**, *11*, 528.
(31) Clark, A. H.; Ross-Murphy, S. B. *Br. Polym. J.* **1985**, *17*, 164.
(32) Tanaka, F.; Ishida, M. *Macromolecules* **1996**, *29*, 7571.
(33) (a) Momii, R. K.; Nachtrieb, N. H. *Inorg. Chem.* **1967**, *6*, 1189. (b) Smith, D., Jr.; Wiersema, R. J. *Inorg. Chem.* **1972**, *11*, 1152. (c) Maya, L. *Inorg. Chem.* **1976**, *15*, 2179. (d) Salentine, C. G. *Inorg. Chem.* **1983**, *22*, 3920.
(34) Flory, P. J. *Principles of Polymer Chemistry*; Cornell University Press: Ithaca, NY, 1953.
(35) (a) Flory, P. J. *J. Am. Chem. Soc.* **1941**, *63*, 3083, 3091, 3096. (b) Stockmayer, W. H. *J. Chem. Phys.* **1943**, *11*, 45. (c) Stockmayer, W. H. *J. Chem. Phys.* **1944**, *12*, 125.
(36) Ishida, M.; Tanaka, F. *Macromolecules* **1997**, *30*, 3900.
(37) Semenov, A. N.; Rubinstein, M. *Macromolecules* **1998**, *31*, 1373.
(38) Rubinstein, M.; Semenov, A. N. *Macromolecules* **1998**, *31*, 1386.
(39) Ide, N.; Tsujii, Y.; Fukuda, T.; Miyamoto, T. *Macromolecules* **1996**, *29*, 3851.
(40) Ide, N.; Fukuda, T. *Macromolecules,* in press.
(41) Ide, N.; Fukuda, T. *Macromolecules* **1997**, *30*, 4268.
(42) Eldridge, J. E.; Ferry, J. D. *J. Phys. Chem.* **1954**, *58*, 992.
(43) Ide, N. et al., unpublished experiments.

MA9805351